In vitro characterization of 6S RNA release-defective mutants uncovers features of pRNA-dependent release from RNA polymerase in *E. coli*

MARIANA OVIEDO OVANDO, LINDSAY SHEPHARD, and PETER J. UNRAU[1]
Department of Molecular Biology and Biochemistry, Simon Fraser University, Burnaby, British Columbia V5A 1S6, Canada

ABSTRACT

6S RNA is a noncoding RNA that inhibits bacterial transcription by sequestering RNA polymerase holoenzyme ($E\sigma^{70}$) in low-nutrient conditions. This transcriptional block can be relieved by the synthesis of a short product RNA (pRNA) using the 6S RNA as a template. Here, we selected a range of 6S RNA release-defective mutants from a high diversity in vitro pool. Studying the release-defective variant R9-33 uncovered complex interactions between three regions of the 6S RNA. As expected, mutating the transcriptional start site (TSS) slowed and partially inhibited release. Surprisingly, additional mutations near the TSS were found that rescued this effect. Likewise, three mutations in the top strand of the large open bubble (LOB) could considerably slow release but were rescued by the addition of upstream mutations found between a highly conserved "-35" motif and the LOB. Combining the three top strand LOB mutations with mutations near the TSS, however, was particularly effective at preventing release, and this effect could be further enhanced by inclusion of the upstream mutations. Overexpressing R9-33 and a series of milder release-defective mutants in *Escherichia coli* resulted in a delayed entry into exponential phase together with a decrease in cell survival that correlated well with the severity of the in vitro phenotypes. The complex crosstalk observed between distinct regions of the 6S RNA supports a scrunching type model of 6S RNA release, where at least three regions of the 6S RNA must interact with $E\sigma^{70}$ in a cooperative manner so as to ensure effective pRNA-dependent release.

Keywords: 6S RNA; transcription regulation; pRNA; *E. coli*; RNA polymerase; regulatory RNA

INTRODUCTION

Escherichia coli 6S RNA binds to σ^{70} RNA polymerase holoenzyme ($E\sigma^{70}$) in low-nutrient conditions and globally suppresses transcription by reducing the amount of free cellular $E\sigma^{70}$ (Wassarman and Storz 2000; Cavanagh et al. 2008). The 6S RNA is released by the synthesis of a short product RNA (pRNA) when optimal nutrient conditions are restored, allowing the bacteria to rapidly resume exponential growth (Wassarman and Saecker 2006; Wassarman 2007; Cavanagh et al. 2012). The transcription of 6S RNA is controlled by σ^{70} (housekeeping gene expression)- and σ^{38} (stationary phase gene expression)-dependent promoters. Since 6S RNA release from $E\sigma^{70}$ depends on nutrient availability, the overall level of free core enzyme (E) is expected to be highly dynamic and largely determined by the turnover rate of the 6S RNA (Hsu et al. 1985; Wassarman and Storz 2000; Kim and Lee 2004; Shephard et al. 2010). This form of RNA-dependent transcriptional regulation, unlike protein-mediated regulation (Jin et al. 2012), is intrinsically rapid and is one of several strategies that bacteria use to promptly respond to changes in their environment (Wassarman 2007). The focus of our investigation is to determine how the 6S RNA sequence contributes to the transcriptional dynamics of RNA polymerase.

A published model suggests that the process of 6S RNA release is analogous to the process of DNA-dependent transcriptional initiation (Panchapakesan and Unrau 2012). During transcriptional initiation, DNA "scrunching" (Cheetham and Steitz 1999) steadily packs downstream DNA into the $E\sigma^{70}$ complex via the ratcheting effect of NTP polymerization (Ederth et al. 2002). The act of scrunching DNA into the polymerase serves to trigger a rearrangement of the polymerase from an initiation complex to an elongation complex capable of processive transcription (Murakami and Darst 2003).

[1]**Corresponding author**
E-mail punrau@sfu.ca
Article published online ahead of print. Article and publication date are at http://www.rnajournal.org/cgi/doi/10.1261/rna.036343.112.

Based on in vitro data, 6S RNA release in the γ-proteobacteria appears to be similar in mechanism to DNA-dependent transcriptional initiation but with pRNA synthesis driving a series of steps that ultimately result in the ejection of the 6S:pRNA complex from E (Fig. 1). After a 9-nt-long pRNA has been synthesized, a release hairpin rapidly forms (Panchapakesan and Unrau 2012). The two arms of the release hairpin are built from highly conserved nucleotides found in the top strand of the large open bubble (LOB) and the top strand residues from the conserved downstream region of the 6S RNA (Fig. 1, state S3). The release hairpin helps to destabilize the RNP complex, resulting ultimately in the ejection of the 6S:pRNA after the pRNA is extended by a further 4 nt (Fig. 1, state S4). Consistent with this model, swapping the downstream top and bottom strands to prevent the formation of the release hairpin slows the 6S RNA release rate, and RNA release is only achieved after the synthesis of a much longer pRNA in vitro (Panchapakesan and Unrau 2012). Interestingly, other bacteria like *Bacillus subtilis* seem to change their secondary structure in the bottom strand of the LOB during release (Panchapakesan and Unrau 2012; Steuten and Wagner 2012), implying that, just as in DNA-dependent scrunching, the mechanism of 6S RNA release is intrinsically flexible and presumably highly dependent on 6S RNA sequence.

To further explore the process of 6S RNA release, we selected a range of *E. coli* release-defective 6S RNA variants using an unbiased in vitro selection approach (Shephard et al. 2010). The types of mutants isolated suggest the existence of several discrete stages in the release process that are consistent with the proposed scrunching model of 6S RNA release (Panchapakesan and Unrau 2012). In the present paper, we focus on the R9-33 isolate due to its ability to remain bound to the $E\sigma^{70}$ in conditions that normally induce very rapid ($t_{1/2} \sim 30$ sec) release of a truncated 6S RNA control construct called T1 (Fig. 2; Supplemental Fig. S1A; Shephard et al. 2010). We uncovered in the R9-33 mutant a surprisingly complex set of interactions between individual point mutations. These interactions triggered two dominant types of release defects determined by the fraction of 6S RNA released and the rate at which this could occur. Some mutants failed to release almost completely, while others released with a broad range of rates, while others released only partially from $E\sigma^{70}$. The nearly complete release defect of R9-33 significantly interfered with *E. coli* survival on LB agar plates and delayed exponential cell growth in LB liquid culture. The fact that only a small number of point mutations in R9-33 are required to produce large changes in 6S RNA release rate highlights how mutation can, in principle, adjust 6S RNA release rate over a huge range of rates, allowing natural selection to fine tune transcriptional control for a wide range of bacterial types and environmental conditions.

RESULTS AND DISCUSSION

In vitro selection of release-defective mutants

A simple 5′ and 3′ truncation of the 6S RNA called T1 (Fig. 2) was previously shown by in vitro selection to contain a "-35"-like region (which plays a central role in RNA binding) and a "-10"-like region that strongly modulates both binding and release (Shephard et al. 2010). A pool of mutants previously selected for its ability to bind $E\sigma^{70}$ (Shephard et al. 2010) was taken forward by four more rounds, this time selecting for binding and no release (Rounds 6–9, Supplemental Fig. S1). Selective conditions were chosen to isolate T1 RNA mutants able to remain bound to the $E\sigma^{70}$ even when incubated under rapid release conditions for periods of time 60 times longer than that required to nearly completely release T1 RNA (rapid release conditions: 250 µM of each NTP, 4 mM $MgCl_2$, for 30 min at 37°C; see Materials and Methods). The fraction of RNA released from each selection round was compared to the control T1 RNA where 8%–11% remained bound to the $E\sigma^{70}$ when incubated under the same rapid release conditions (Supplemental Fig. S1B, blue bars). After the first round of selection for release-defective mutants, only 10% of the RNA population remained bound to the $E\sigma^{70}$ after incubation in fast release conditions (Supplemental Fig. S1B, red bars). The fraction bound increased to 38% by Round 7, 65% by Round 8, and stabilized at 63% by Round 9; at this point, the selection was stopped, and pool isolates were characterized.

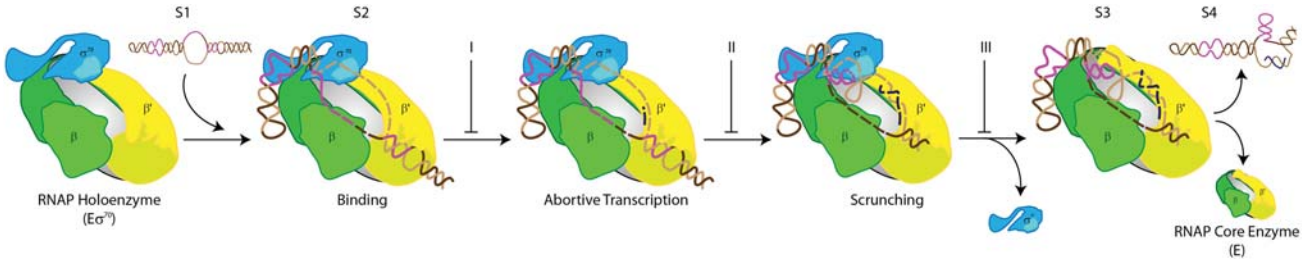

FIGURE 1. Major proposed steps of *Escherichia coli* 6S RNA release. Highly conserved areas in the 6S RNA are shown in purple; the template strand is in light brown and nontemplate RNA in dark brown. A product RNA (pRNA) is shown in dark blue and triggers the formation of a release hairpin formed from the conserved "-10" region and the top strand of the downstream helix. Based on the scrunching-dependent release model for 6S RNA (Panchapakesan and Unrau 2012).

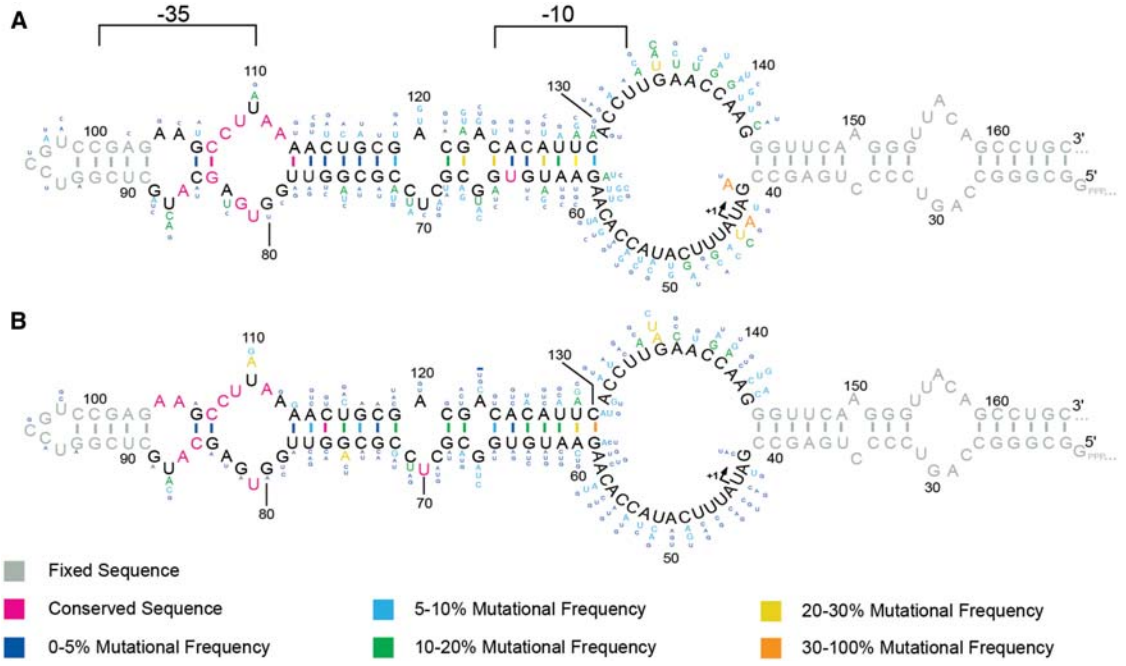

FIGURE 2. Round 9 release-defective 6S RNA consensus compared with binding and release selection. (*A*) Consensus sequence based on 71 variants from the binding and no release selection performed in this study. The "-35" sequence is conserved in 6S RNA release-defective mutants. Significant changes away from the biological consensus were found in the vicinity of the pRNA TSS (noted by arrow). (*B*) Consensus sequence based on 60 variants from a previous binding and release selection (Shephard et al. 2010). Black residues were deliberately mutagenized in the initial pool synthesis and were found to vary. Purple residues were completely conserved after the selection. Nucleotide variants and base-paired residues are color coded according to the observed percentage of mutational frequency.

Release-defective mutants were found during the in vitro selection

Seventy-one isolates were cloned and sequenced from Round 9 of the release-defective selection. Aligning these release-defective sequences revealed a pattern of nucleotide conservation (Fig. 2A) that could be compared to the one observed in our previous selections for binding- and release-competent 6S RNA mutants (Fig. 2B; Shephard et al. 2010) or to the phylogenetically conserved pattern found in nature (Supplemental Fig. S2). We focused on positions with mutational frequencies significantly different from the 10% frequency initially built into the starting pool (Supplemental Table S1), with the expectation that regions of high sequence conservation or regions of hypermutability would be correlated with release defects.

When aligned, 9 nt located within the "-35" sequence island were found to be absolutely conserved (Fig. 2A). The probability that any one such location was conserved by chance alone was only ~0.06% (i.e., 0.9^{71}, where 0.9 corresponds to the probability of finding the wild-type sequence in the starting pool). Notably, the pattern of absolute sequence conservation was shifted by two residues toward the LOB of the 6S RNA relative to the pattern observed in both our binding and release selection (Fig. 2) and the pattern of sequence conservation found in nature (Supplemental Fig. S2B). The shift in conservation pattern was accompanied by the presence of absolute base-pairing between residues 78 and 113. This base-pairing pattern was not found in the binding and release selection but was found in the selection for binding (Shephard et al. 2010), suggesting that pairing position 78 to 113 helps to stabilize the 6S:Eσ^{70} complex. Residues 83, 87, and 110, located in the "-35" region of high sequence conservation, remained highly variable in all in vitro selections as well as in the natural phylogeny, suggesting that these residues do not make specific contacts with Eσ^{70} upon binding.

According to our in vitro selection results, the top strand of the 6S RNA LOB could be divided into two distinct regions based on its sequence conservation. Region 131 to 134 corresponds to residues that can form the base of the release hairpin's left arm and are highly conserved in the natural phylogeny (Supplemental Fig. S2B). During the release-defective selection, the region 131–134 exhibited a relatively high level of sequence conservation, having an overall mutational frequency of 5.6% per residue relative to the original frequency of 10% found in the unselected pool population (Supplemental Table S1). This data suggests that the region cannot be easily changed and is consistent with previous findings that indicate that the region has a complex effect on release rate (Shephard et al. 2010). In contrast, the region from positions 135 to 141, which forms the upper part of the predicted release hairpin's left arm (Panchapakesan and Unrau 2012), had a significantly higher mutational frequency of

26.2% in the release-defective selection. It is particularly striking that, without exception, the dominant mutation at each position in this region is a transversion (Fig. 2A), which would be predicted to weaken the formation of the release hairpin and could, therefore, be predicted to delay or preclude 6S RNA release.

The selection for release defects produced strong deviations from both the wild-type consensus sequence and previous selections for binding and release (Shephard et al. 2010) in the vicinity of the transcription starting site (TSS, residue U44) (Fig. 2). Mutations G42A, U44A (the TSS), A45U, and, to a lesser extent, U47G and C49G, had high statistical significance in our selection and were observed significantly more often than expected by chance alone (Supplemental Table S1). These findings agree with previous data on the importance of the TSS region for efficient pRNA production. However, our in vitro selection for release-defective variants indicates that Eσ^{70} has a strong preference for initiating with an A, in contrast to initiation in wild-type sequences where Eσ^{70} shows no preference for a specific nucleotide (Cabrera-Ostertag et al. 2013). The remaining nucleotides in the bottom strand (positions 50–61) of the LOB were found to vary at a frequency close to the original frequency of the pool. Based on these statistics, the TSS region was implicated in 6S RNA regulation, presumably by controlling pRNA synthesis, as previously speculated by others (Wassarman and Saecker 2006).

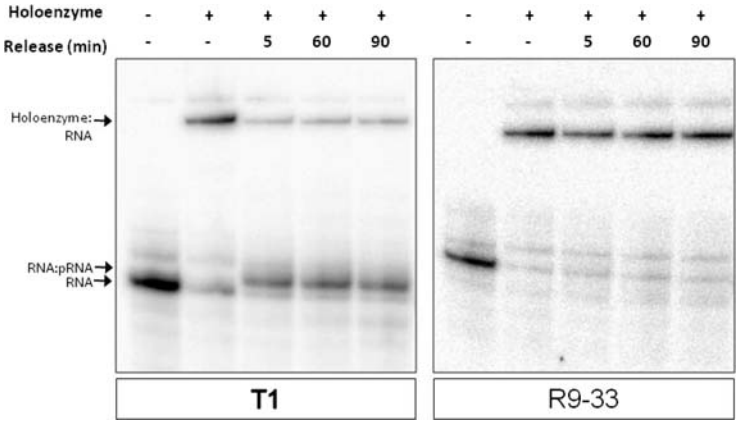

FIGURE 3. R9-33 mutant 6S RNA fails to release from Eσ^{70}. Binding and release capabilities were tested for different constructs and compared to the T1 RNA. Body-labeled RNA (*left* lane, both panels) was incubated with Eσ^{70} (second lane of each panel), and rapid release was induced by the addition of $MgCl_2$ and NTPs. Time points were taken at 5, 60, and 90 min. The mobility difference between mutant RNA and the RNA:pRNA complex is indicated with black arrows.

Several classes of mutant 6S RNA release defects were found

The scrunching model predicts that release-defective 6S RNA mutants could result from failures at major steps in the release process (Fig. 1). Sequences from 71 clones from Round 9 were sorted using a pair-wise alignment approach (Supplemental Fig. S3). Only weak clusters of sequence similarity were found, and 13 clones that spanned the resulting distance tree were tested in vitro for their binding and release properties. Constructs R9-1 and R9-8 were most closely related to the T1 construct and consistently were the fastest mutants to release from the Eσ^{70}. Even so, R9-1 and R9-8 were 15 and 60 times slower to release than the T1 construct (Supplemental Figs. S3–S5). The remaining 11 isolates released even slower or almost completely failed to release after 90 min of incubation under rapid-release conditions (Fig. 3; Supplemental Fig. S4). While the sequence of the short pRNAs produced by each of the thirteen clones was not explicitly determined, the product bands observed for each correlated well with the template TSS sequence. To detect the products of Eσ^{70} activity, newly synthesized RNAs were labeled with either [γ-^{32}P]-ATP or [α-^{32}P]-UTP. The new RNAs were compared to the 13-nt pRNA from T1 RNA (Supplemental Fig. S6) and distinguished from contaminant bands found to originate from the radioisotope source vials (see Materials and Methods). The products of synthesis where classified as either short pRNAs (typically 2–8 nt) or pRNAs (13 nt and longer). Based on the patterns of pRNA synthesis, the release-defective RNAs were grouped into three major classes.

The most common class I (R9-70, -52, -44, -62, -18, and -33) produced very low amounts of full-length pRNA and synthesized either apparently normal (R9-33, -18, -62, -70) or low amounts of short pRNA (R9-52 and -44) relative to the T1 RNA reference construct (Supplemental Fig. S6). Constructs R9-18 and -62 have a similar sequence in the TSS region (5′…$A_{42}A_{43}\mathbf{U_{44}}(C_{45}/U_{45})U_{46}$…, predicted TSS in bold) and share a similar short pRNA pattern, suggesting that both synthesize products with sequence **A**U, **A**UU, etc. (Supplemental Fig. S6). Construct R9-33 has a unique template sequence (5′…$G_{42}A_{43}\mathbf{A_{44}}U_{45}U_{46}$…) and produced a labeled dinucleotide only with [α-^{32}P]-UTP present, consistent with the predicted A_{44} TSS. R9-33 was characterized in greater detail because, after 90 min of incubation under rapid release conditions, on average 85% of initially bound RNA remained attached to the Eσ^{70} (Fig. 3), the highest of any mutant tested.

Class II (R9-24), was capable of producing very long pRNAs that labeled strongly with [α-^{32}P]-UTP but not with [γ–^{32}P]-ATP (Supplemental Figs. S6,S7), while exhibiting a very slow release rate (Supplemental Fig. S4). The sequence for R9-24 in the TSS region is 5′…$A_{42}A_{43}\mathbf{A_{44}}A_{45}A_{46}U_{47}U_{48}$…, which suggests that this construct can act as a template for the production of oligo (U) containing pRNA. However, during nucleotide feeding experiments (Supplemental Fig. S8), pRNA production was not observed when only UTP was used, suggesting that the long polymer produced by R9-24 is either not entirely composed of poly (U) or that additional

nucleotides are required to stabilize the polymerization of UTP. We speculate that R9-24 remains bound to the Eσ^{70}, due to a template slippage type mechanism. Further work is required to characterize the pRNA synthesis mechanism from this unusual sequence.

Class III (R9-8, -1, -34, -11, and -66) produced pRNAs that were as long or longer than the T1 pRNA and released from Eσ^{70}, albeit 10 to 100 times slower than the T1 control (Supplemental Figs. S5,S6). Within this class, R9-1 and -8 had an identical template sequence of 5′…$G_{42}A_{43}\mathbf{U_{44}}U_{45}U_{46}U_{47}U_{48}$…, and both produced short pRNAs (2–8 nt long) with an intensity and band pattern identical to the short pRNAs produced by T1 RNA that happens to share a similar template sequence (5′…$G_{44}A_{43}\mathbf{U_{44}}A_{45}U_{46}U_{47}U_{48}$…). On the other hand, R9-11 and -34 (5′…$A_{42}A_{43}\mathbf{U_{44}}A_{45}U_{46}[U_{47}/C_{47}]$…) produced copious amounts of short RNA. These constructs, just like the T1 RNA, conserve the A45 residue, which may be of significance. The efficient production of short RNA, therefore, seems to be strongly modulated by the sequence immediately surrounding the TSS (Cabrera-Ostertag et al. 2013). While this class was not studied in further detail, its phenotype of long pRNA production and slow release rate seems very similar to that of a construct where the downstream top and bottom strands were swapped to prevent the formation of the release hairpin (Panchapakesan and Unrau 2012).

Complex, synergistic effects between point mutations in the R9-33

Since R9-33 was the most release-resistant variant found in this screen, we decided to explore which of its mutated residues most heavily influenced release from Eσ^{70}. Systematically adding the substitutions present in R9-33 back into the T1 RNA scaffold produced two significant phenotypes: a slowdown in the release rate or a failure to release from the Eσ^{70}. Often failure to release was not complete, and thus, combinations of the two phenotypes were commonly observed. While a slowdown in release can be explained by a single rate-limiting step in the process of 6S RNA release, a partial release defect implies a more complex failure mechanism, suggestive of a multistep process.

The R9-33 sequence differs from the T1 RNA by a total of 16 nucleotide substitutions (Fig. 4A). Ten of these mutations were found in upstream regions of the 6S RNA that are weakly conserved either in nature or in selections for binding and

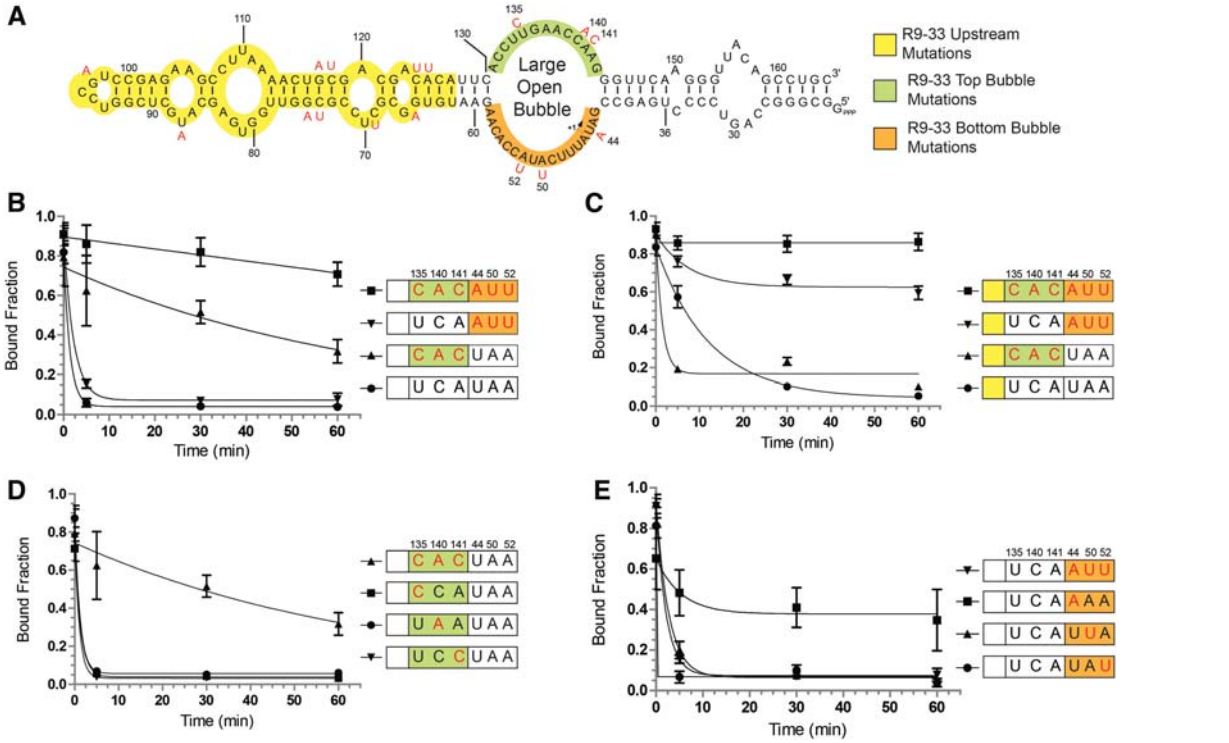

FIGURE 4. Substitutions around the large open bubble (LOB) of R9-33 act in a highly synergistic manner and are responsible for blocking release from Eσ^{70}. (*A*) T1 RNA sequence is noted in black while substitutions found in R9-33 are in red letters. The molecule was divided into three distinct zones: a yellow upstream region that contains 10 mutations; a green top strand in the LOB region contains three substitutions at positions 135, 140, and 141; an orange bottom strand in the LOB contains three substitutions at positions 44, 50, and 52. (*B*) Release kinetics for T1 RNA and three other constructs with triple mutations (in red letters). (*C*) Release kinetics for R9-33 constructs with substitutions that were sequentially removed according to the color code described in panel *A*. (*D*) Release kinetics for constructs with point mutations (in red letters) in the top strand of the 6S RNA LOB. (*E*) Release kinetics for constructs with point mutations (in red letters) in the bottom strand of the 6S RNA LOB. Error bars correspond to standard deviations about the mean of at least three independent experiments.

release (Shephard et al. 2010). Eight of these mutations were found between the "-35" region and the LOB (Fig. 4A, residues in red, yellow region). Interestingly, these mutations substantially preserve the predicted secondary structure in this region: Four of these eight mutations replace two wild-type G:C pairs with new A:U pairs. C69U is not predicted to be in a base-pairing region, while G75A repairs a G:U wobble pair, and C74U creates an adjacent wobble pair. Only A125U would be predicted to destabilize the predicted upstream secondary structure, and this mutation creates a potential U:U mismatch. Further upstream, only two mutations were found: The U87A mutation is located at a position that both in nature and in all of our artificial selections was highly variable (Fig. 2; Supplemental Fig. S2). Further, the G97A mutation is located in a region known to be dispensable for 6S RNA release (Shephard et al. 2010). The remaining six mutations were split evenly between the top strand of the LOB (green region, Fig. 4A), and the bottom strand of the LOB (orange region, Fig. 4A). The top strand mutations U135C and C140A would be predicted to interfere with changes in RNA secondary structure that occur during pRNA-induced hairpin formation, while the bottom strand U44A mutation is located at the predicted TSS and could easily influence 6S release kinetics.

Top and bottom strand LOB mutations together were required for a strong release defect to manifest, and this phenotype was enhanced in a complex way by the inclusion of the upstream mutations. The triple substitutions in either the top or bottom strands of the LOB were found to slow down release (Fig. 4B, inverted triangles and triangles) 25- and twofold, respectively (Supplemental Table S3), compared to the T1 sequence (circles). However, when all six substitutions around the LOB were combined, we observed an almost complete failure to release (Fig. 4B, squares). Like the top and bottom strand mutations, the presence of only the 10 upstream mutations (Fig. 4A, yellow region) was found to slow release rate by 10-fold (cf. Fig. 4C,B, circles). Interestingly, these upstream mutations could behave in a synergistic or antagonistic manner with mutations found in the LOB. When the 10 upstream mutations were combined with bottom strand LOB mutations, ~30% of the RNA released at a rate eight times slower than the T1 reference sequence. The remaining ~60% of the mutant RNA released at a substantially slower rate (cf. Fig. 4C,B, inverted triangles). Conversely, the combination of upstream mutations and top strand LOB mutations resulted in release at a rate similar to that found for the top strand LOB mutations by themselves, but in this case, ~15% of the mutant RNA population released at a considerably slower rate (cf. Fig. 4C,B, triangles). When the upstream mutations were combined with mutations in the top and bottom strands of the LOB to recreate the full R9-33 construct, the full release defect was observed as expected. It is clear from these observations that complex interactions among these three distinct regions of the 6S RNA molecule serve to control major events that occur during 6S RNA release.

While the complete set of point mutations in the top and bottom strands could trigger major changes in release rates, the individual point mutations generally did not trigger major changes in release rate or result in a partial failure to release. Point mutations U135C (Fig. 4D, squares), C140A (circles), and A141C (inverted triangles) did not by themselves change release rates significantly. However, when the three mutations were combined as discussed previously (Fig. 4D, triangles), release was slowed 25-fold compared to T1, suggesting that a release defect on the top strand demands synergistic effects among the three residues.

In contrast to the top strand mutations, where all three substitutions were required for a release defect to manifest, mutation of some bottom strand residues could suppress a release defect induced by mutating the TSS. By itself, the U44A mutation resulted in a strong release defect, where ~40% of the mutant RNA remained bound (Fig. 4E, squares). This was surprising, as the triple mutant on the bottom strand (inverted triangles) released only twofold slower than the T1 construct. To explore this further, we constructed an A50U mutant (triangles) which released only 2.5-fold slower than T1, while the A52U mutant (circles) released with a rate very similar to that of the T1 construct. The marginal effect that A50U and A52U had on release rate makes it hard to understand how these two mutations, when combined with the U44A mutation, can nearly completely rescue the release defect induced by U44A on its own.

Effects of in vivo expression of mutant 6S RNAs

Our in vivo expression studies found that mutant 6S RNAs inhibit bacterial growth and decrease cell viability in high-nutrient conditions. In vitro studies provided us with a set of 6S RNA variants that can bind and sequester $E\sigma^{70}$ just like the endogenous 6S RNA but with varying release rates. The best release-defective mutant R9-33, together with the T1 RNA and a mutagenized 6S RNA with low affinity to $E\sigma^{70}$, were cloned into a modified pEcoli-Cterm 6xHN (Clontech) vector driven by a T7 promoter (Supplemental Fig. S10). This type of strongly inducible system used for expressing our mutants allowed us to draw conclusions from early time points where strong expression of plasmid-derived RNA was verified by Northern blot. The RNA transcribed in vivo from pEcoli-R9-33, and pEcoli-T1 DNA (due to the presence of the *lac* O and terminator), were longer than the R9-33 and T1 RNA (143 nt), but in vitro they showed the same binding and release capabilities as their shorter counterparts, shown in Figure 3. When tested in vitro for binding and release, the RNA transcribed from pEcoli-LowBinder DNA produced a slower mobility band relative to bound T1 RNA and did not show any evidence of pRNA-dependent release. The same LowBinder RNA could be displaced from $E\sigma^{70}$ by T1 RNA during in vitro competitions assays (data not shown). For all of these constructs, induction of the chromosomally expressed T7 RNA polymerase by IPTG

served to decouple (for the lifetime of T7 RNA polymerase) the transcription of mutant RNAs from the activity of bacterial $E\sigma^{70}$.

Delay in cellular growth correlates with severity of mutant phenotype

Expression of pEcoli-LowBinder, pEcoli-T1, and pEcoli-R9-33 resulted in a variety of growth patterns that could be correlated well with the in vitro behavior of each construct. Freshly transformed cells were grown overnight in LB+Amp, diluted 200-fold the next day and induced with IPTG immediately after dilution. When grown in the absence of IPTG, all transformed cells grew at the same rate as untransformed cells grown in LB (Fig. 5A, squares and empty circles; data not shown). When induced with IPTG, *E. coli* transformed with the different plasmids showed clear evidence of unbalanced growth which is reflected in changing rates of growth during the exponential phase. In contrast, uninduced cells showed a constant rate of cell division during exponential growth. The pEcoli-LowBinder (Fig. 5A, diamonds) and pEcoli-T1 (inverted triangles) cells grew slower than the wild type, and their growth curves presented three different growth rates prior to entering stationary phase. Growth for pEcoli-R9-33 (triangles)-transformed cells also showed three different slopes, and growth was minimal until ~300 min post-induction, when they reached a growth rate similar to that of uninduced or wild-type cells. A fourth control construct, pEcoli-empty (self-ligated double-digested vector), grew like untransformed cells, suggesting that the expression of mutant 6S RNA was responsible for the slowdown in growth (data not shown). These data, particularly at early time points, suggests that pEcoli-R9-33 expression significantly inhibits cell growth even in high-nutrient conditions.

To explore the hypothesis that cells expressing pEcoli-R9-33 plasmid-derived RNA also had a lowered viability, aliquots of uninduced exponentially growing cells were plated onto LB+Amp agar with or without IPTG (Fig. 5B). The percentage of cells able to form colonies (CFU) was calculated relative to cells transformed with pEcoli-Empty, which had an absolute colony forming potential of 85% (colonies formed on +IPTG plates relative to −IPTG plates). Cells transformed with pEcoli-LowBinder and grown on +IPTG agar showed a CFU ability of 82% relative to the pEcoli-Empty control, suggesting that the majority of these cells remained viable upon IPTG induction. In contrast, only 2.6% of the cells transformed with pEcoli-T1 formed colonies, implying that high levels of 6S RNA expression either prevents cell division and/or potentially causes cell death. Strikingly, cells transformed with pEcoli-R9-33 exhibited survival rates of only 0.2%. The fact that both the colony-forming ability and the altered growth observed in liquid media correlate with the in vitro phenotypes of each RNA construct suggests that inhibition of transcription by either T1 or mutant 6S RNA expression is at the root cause of these phenotypes.

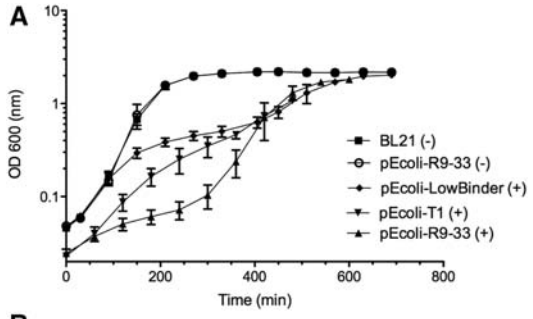

B

Construct	CFU Relative to pEcoli-Empty
pEcoli-Empty	100.0
pEcoli-Low binder	82.2
pEcoli-T1	2.6
pEcoli-R9-33	0.2

FIGURE 5. Bacterial overexpression of mutant 6S RNA produces growth defects and correlates with in vitro release defects. (*A*) Growth curves for *E. coli* BL21 (DE3) cells transformed with one of the following plasmid vectors; pEcoli-LowBinder, pEcoli-T1, or pEcoli-R9-33. Cells were grown in LB+Amp (100 µg/mL) and 5 mM IPTG (+ symbols) from the time of inoculation. Cells transformed with pEcoli-R9-33 but grown in the absence of IPTG (− symbols) were used as a control together with untransformed BL21 cells grown in LB broth. (*B*) Expression of mutant RNA correlates to cell survival and growth. Exponentially growing cells ($OD_{600} = 0.7$) in LB+Amp were plated onto LB+Amp agar with and without 5 mM IPTG. The percentage of CFU was calculated for each construct and expressed as a percentage of survival normalized to that of the pEcoli-Empty. The control plasmid pEcoli-Empty grew like pEcoli-R9-33 – IPTG in LB+Amp liquid culture (data not shown in panel *A*). Error bars correspond to standard deviations from the averages of three independent experiments.

T1 and R9-33 RNAs initially strongly expressed in vivo

In order to track mutant RNA expression in vivo, total RNA was extracted from cells grown in LB+Amp in the presence or absence of IPTG. Equal amounts of total RNA were loaded onto denaturing polyacrylamide gels and analyzed. Plasmid-derived RNA and endogenous 6S RNA (184 nt) could be visualized by SYBR Green staining and observed band patterns confirmed by Northern analysis (Fig. 6A). T1 and R9-33 RNA were synthesized in vitro using plasmids digested with ClaI as template (pcT1 and pcR9-33) and used to control for probe specificity and the size of the plasmid-derived RNA. The two bands observed in the plasmid cut lanes (pcT1 and pcR9-33) correspond to the RNA produced by runoff transcription (top band, 226 nt long that includes the operator and terminator sequences in the vector) (Supplemental Fig. S10) and the termination at the appropriate site (bottom band). Levels of endogenous 6S RNA were low at early time points for all the cells. In the case of cells transformed with pEcoli-R9-33, plasmid-derived RNA production was the highest 120 min after induction and decayed steadily to very low levels after 400 min of growth. This decay is in agreement with the time when cells entered their fastest growth (Fig. 6A). The ratio of

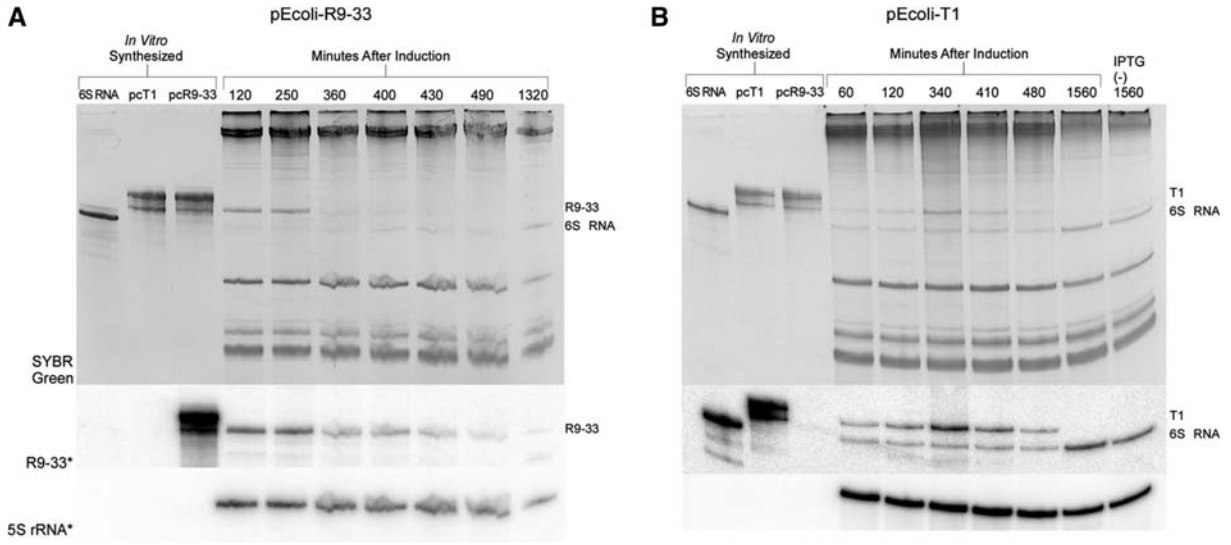

FIGURE 6. Northern analysis of in vivo mutant 6S RNA expression. (*A*) Total RNA was extracted from *E. coli* pEcoli-R9-33 cells under denaturing conditions. Five OD_{600} units were taken starting at 60 min of incubation in LB+Amp with IPTG and at intervals until 1320 min (22 h). An 8% denaturing PAGE gel imaged by SYBR Green is shown in the *top* panels. On the *left*, in vitro-synthesized 6S RNA was loaded alongside in vitro-transcribed T1 and R9-33 RNA (using plasmid cut [pc] with ClaI as DNA template) that served as a control for probe specificity and also as size reference for plasmid-derived RNA. The nucleic acid in this gel was transferred onto a membrane and probed with radiolabeled R9-33-specific probe (*middle* panel; Supplemental Table S2). (*B*) Total RNA was extracted from BL21 pEcoli-T1 cells using previously described conditions. The same positive controls were loaded in this gel along with a sample extracted from BL21 pEcoli-T1 cells grown in the absence of IPTG. In all cases, hybridization to 5S rRNA was used as an internal loading control (*bottom* panels).

R9-33 to 6S RNA, as quantified by SYBR Green staining, ranges from 10 to 1 at 120 min to an almost equal ratio at 400 min after induction, suggesting that the initial high concentrations of R9-33 are responsible for growth inhibition at early times. Expression of pEcoli-T1 RNA peaked at ~340 min and gradually decayed until it could not be detected at 1560 min (stationary phase) as monitored by a Northern probe able to detect both pEcoli-T1 and endogenous 6S RNA simultaneously (T1* probe) (Fig. 6B).

To verify that plasmid-derived RNA binds to cellular $E\sigma^{70}$, whole-cell extracts from +ITPG cultures grown for 180 min were prepared and tested by Northern blot. Plasmid-derived R9-33 RNA forms a complex (Supplemental Fig. S10, right lane) with a similar native gel mobility to that of a complex prepared from commercial $E\sigma^{70}$ (Epicentre) and in vitro-transcribed R9-33 RNA (Supplemental Fig. S10, left lane). The slow mobility band on the Native lane (Supplemental Fig. S10) was only 24% of the total signal, which suggests that the strong expression of plasmid-derived R9-33 RNA triggered by IPTG induction effectively inhibited all bacterial $E\sigma^{70}$ transcription.

CONCLUSION

The release-defective mutants isolated from a high-diversity RNA pool could be sorted into three classes, each with a distinct pRNA synthesis profile. The different classes of release-defective mutants appear to correspond to stalls in different stages of a previously modeled 6S RNA release process (Panchapakesan and Unrau 2012). In class I mutants, the accumulation of substitutions around the "-10" and TSS regions allows the synthesis of short pRNAs while suppressing the synthesis of longer pRNAs that appear to be required for wild-type 6S RNA release. Based on the "scrunching" model shown in Figure 1, longer pRNAs are thought to be required after binding to transition successfully from State 2 (S2) to State 3 (S3). The class II (R9-24) mutant further supports this idea. In contrast to the class I mutants, the class II mutant makes a very long pRNA, while also failing to release. We speculate that template slippage prevents the accumulation of the mechanical force required to scrunch the RNA into the $E\sigma^{70}$ complex and would, in our interpretation, also correspond to an inability to transition from the S2 to the S3 state (Fig. 1). Slippage with shifts of −1 or −3 nt have previously been shown to help stabilize the DNA:$E\sigma^{70}$ complex during transcriptional initiation (Borukhov et al. 1993; Liu and Martin 2009), so it is possible that a similar stabilization occurs in this 6S RNA mutant. The third class (III) of release-defective mutants makes longer than expected pRNAs and has a phenotype consistent with a failure to leave either the intermediate scrunched state or the S3 state formed after the release of σ^{70} (Fig 1). It is hypothesized that the mutations in this group allow for stronger interactions between the RNA and the $E\sigma^{70}$ and that a longer than usual pRNA is required to create enough strain in the 6S: $E\sigma^{70}$ complex to trigger full 6S RNA release.

The presence of mutations that only partially release is consistent with a 6S RNA release model where intermediate

structural states of either the 6S RNA or 6S:Eσ^{70} might become "jammed" during pRNA synthesis. Interestingly, for the R9-33 mutant, the "jamming" was enhanced by the inclusion of upstream mutations (Fig. 4, yellow region). Previously, we have shown that the "-35" sequence region plays an essential role in initial RNA binding (Shephard et al. 2010). Upstream sequence conservation showed a systematic shift toward the LOB in our selection (Fig. 2), suggesting that mutant RNAs bind Eσ^{70} in a distinctly different fashion than wild-type 6S RNA. A recent 6S RNA model docked to RNA polymerase based on the crystal structure of the bound open form DNA:Eσ^{70} (Murakami and Darst 2003; Steuten et al. 2013) suggests that upon initial binding, the 6S RNA interacts not only with $\sigma^{70}_{4.2}$, but also with $\sigma^{70}_{2.1}$, $\sigma^{70}_{2.3}$, $\sigma^{70}_{3.1}$, and $\sigma^{70}_{3.2}$. This model would predict that eight out of 10 mutations (G65A, C69U, C74U, G75A, G117A, C118U, C124U, and A125U) located in the upstream region of R9-33 are in the immediate vicinity of $\sigma^{70}_{2.1}$ (closer to the "-10" area) and $\sigma^{70}_{3.1}$ that stretches between the "-10" and "-35" regions (Steuten et al. 2013). If these mutations stabilize interactions between the 6S RNA upstream region and the distal σ^{70} domains, they might serve to inhibit changes in σ^{70} structure that we postulate are required to trigger normal 6S RNA release. This inhibition of structural change could, therefore, lead to jamming of a stochastically determined subset of mutant RNAs during the process of scrunching-mediated release.

Mutations within the top strand LOB cause complex release defects that are indicative of RNA structural dynamics and enzyme kinetics that are only partially understood. Our model of 6S RNA release suggests that the formation of a 9-bp release hairpin in the top strand plays an important role in normal 6S RNA release (Panchapakesan and Unrau 2012). U135C and C140A mutations, which disrupt this helix, might, therefore, be expected to have an effect on release rate. We, however, could not detect the effect of either mutation on release rate, and it was only when A141C was included in addition to these two mutations that an observable release defect was observed (Fig. 4D). Each mutation would be expected to create either a bulge (U135C or C140A) or a change in the tri-loop sequence (A141C) and might, therefore, not significantly change the thermodynamics of release hairpin formation individually. Combined, these mutations might have three effects, the first, as previously mentioned, being thermodynamic. A second and hard to determine consequence of these mutations is that they may alter contacts formed transiently with Eσ^{70} so as to slow the mechanism of release. While this cannot be precluded, we note that the lack of sequence conservation observed in the top strand of the TSS in our phylogeny (Fig. 2) implies that there is no unique sequence capable of achieving such a state of affairs. The third and, we think, most significant factor concerns the register of the right arm of the release hairpin that forms during pRNA synthesis. It is notable that R9-33 accumulates a pRNA that is ~6 nt long, in contrast to either the T1 control or to Class III mutants which can rapidly synthesize pRNAs $\geq$13 nt long (Supplemental Fig. S6). After synthesizing a pRNA 6 nt long (i.e., with sequence 5′-UUCGGC), R9-33 nucleotides on the top strand that were originally paired to the bottom template strand are now free to start forming the release hairpin by pairing with their reverse complements found in the top strand "-10" region. The C140A and A141C mutations seem ideally located to shift this pairing so as to make the formation of a full release hairpin nearly impossible: A141C can now pair potentially with G145, which, in this new register, would favor the pairing of C140A with U146, at which point further stem formation would be strongly disfavored, as C139 would not pair with U147. Based on our data, we, therefore, favor a model where top strand LOB mutations found in R9-33 markedly interfere with the formation of the release hairpin and hence serve to help delay mutant 6S RNA release.

The mutations near the TSS on the bottom strand of the LOB are more challenging to explain. Not surprisingly, U44A causes a marked decrease in transcriptional initiation efficiency, as has been noted for many DNA TSS, and appears most likely to be a consequence of the enzyme active site favoring initiation with ribopurines (Revyakin et al. 2006). How adjacent mutations close to the TSS can abolish this effect remains to be explained (Fig. 4E), but it is striking that such mutations, when combined with top strand mutations, are sufficient to produce a strong release defect (Fig. 4B,C, squares). These findings complement the work of Cabrera-Ostertag et al. (2013), where variation of the TSS regions was previously explored.

E. coli cells expressing R9-33 confirmed its potent regulatory ability, previously observed in vitro, by delaying entry into exponential growth and preventing colony growth. Although strong overexpression is not the ideal system to test 6S RNA mutants in vivo since it allows many potentially conflicting variables during late induction, at short times the high induction of mutant RNAs should be suggestive of the 6S RNAs ability to regulate the transcription dynamic in high-nutrient conditions. Our findings are in broad agreement with previous data on expression of mutant 6S RNA in *E. coli* and *B. subtilis* (Cavanagh et al. 2012). The marked cell death and inhibition of growth observed with overexpression of R9-33 and the decreasing trend in this respect seen with T1 RNA and control RNAs with even weaker binding interactions to Eσ^{70} indicate that, even in high-nutrient conditions, RNAs that interact with bacterial RNA polymerase can have a significant effect on growth dynamics.

The large range of release defective sequences found in this study implies that many sequences close to the 6S RNA sequence are avoided by natural selection because they do not exhibit correct pRNA-induced release from Eσ^{70} and can, like the R9-33 submutants characterized in this study, become jammed during release. Interactions between the top and bottom regions of the LOB and with upstream 6S RNA sequence are strongly implied by the study of such jammed mutants, and how such interactions feature in

normal 6S RNA release is still an open question. Further study of different classes of jammed states appears likely to improve our understanding of both 6S RNA release and nucleic acid scrunching in bacterial RNA polymerases.

MATERIALS AND METHODS

Library preparation and in vitro selection

The starting pool was the Round 5 population of 6S RNA mutant sequences previously selected for their ability to bind to $E\sigma^{70}$ (Shephard et al. 2010). During four additional rounds of selection, 6S RNA mutant sequences were selected for their ability to bind and not be released from $E\sigma^{70}$ (Supplemental Fig. S1A) using the following protocol: DNA from the previous round of selection was transcribed and the resulting RNA gel-purified. Pool RNA at 250 nM was treated as described in the following section. One volume of native loading buffer (50% glycerol, 0.025% xylene cyanol, 0.025% bromophenol blue) was added, and complexes were resolved by native 5% (37.5:1 acrylamide:bis) PAGE run at 4°C. The shifted band corresponding to the T1:$E\sigma^{70}$ complex was then carefully excised and the bound RNA recovered. RNA was eluted overnight (300 mM NaCl, 4°C) and recovered by ethanol precipitation. Using this RNA, the general binding and release was repeated and samples loaded onto a native 5% PAGE. RNA bound to $E\sigma^{70}$ was again recovered before being reverse-transcribed. After treatment with 100 mM KOH for 10 min at 90°C, the resulting cDNA was neutralized with 100 mM Tris-HCl and PCR-amplified for the next round of selection (Supplemental Fig. S1A).

General 6S RNA binding and release

The same approach was used during the in vitro selection and testing of individual mutant constructs. In vitro-transcribed 6S RNA (250 nM), ^{32}P-labeled and PAGE-purified (50 mM Tris-HCl at pH 7.9, 5 mM DTT, 2.5 mM spermidine, 26 mM $MgCl_2$, 0.01% Triton X-100, 8 mM GTP, 5 mM ATP, 5 mM CTP, 2 mM UTP, α-[^{32}P]-UTP template DNA at ~100 nM, 5 units/μL T7 RNA polymerase), was mixed with RNA Buffer (20 mM HEPES pH 7.5, 5 mM $MgCl_2$), heated to 80°C for 2 min, and cooled to 50°C for 5 min. Next, RNA was bound to 200 nM *E. coli* RNA polymerase holoenzyme ($E\sigma^{70}$, Epicentre) in 15 mM HEPES at pH 7.5, 90 mM KCl, 0.75 mM DTT, 75 μg/mL heparin at 37°C for 30 min. Release from $E\sigma^{70}$ was initiated by the addition of 250 μM of each NTP and 4 mM $MgCl_2$ while incubating at 37°C. When individual constructs were tested, time points were taken between 1 and 90 min to differentiate between constructs that release slowly from those that fail to release. During in vitro selection, the RNA pool was incubated for 30 min with 250 μM of each NTP and 4 mM $MgCl_2$ at 37°C. Reactions were quenched by the addition of 2× native gel loading dye and resolved in a 5% native gel.

In vitro transcription using 6S RNA as template

"Cold" T1 RNA construct and release-defective variants were in vitro-synthesized as described above. A final concentration of 250 nM "cold" RNA was bound to the $E\sigma^{70}$ as described in the previous paragraph. Release was induced with a mix of 250 μM of each NTP, 4 mM $MgCl_2$, and spiked with 25 μCi of [α-^{32}P]-UTP or [γ–^{32}P]-ATP to radiolabel nascent RNA for 30 min. Reactions were quenched by the addition of 2× denaturating loading dye (see above) and resolved in a 23% denaturing PAGE (Supplemental Figs. S5–S8). To confirm that the product RNA observed was derived from $E\sigma^{70}$, time courses were performed with and without mutant 6S RNA and using either [α-^{32}P]-UTP (Supplemental Fig. S7) or [γ-^{32}P]-ATP (Supplemental Fig. S8). Control experiments were set up to distinguish between the specific products of polymerization, contaminants from the radiolabeled NTPs, or intrinsic polymerase activity. The nucleotides [α-^{32}P]-UTP and [γ-^{32}P]-ATP were incubated in the same buffer as the transcription assay and resolved in denaturing gels (Supplemental Figs. S8,S9), and the contaminant bands were indicated in Supplemental Figure S6 with star symbols. In addition, one reaction was set up without RNA template in it (Supplemental Fig. S8), and as expected, no polymerization was seen. All in vitro template sequences were verified by sequencing prior to use.

6S RNA mutant plasmid construction

DNA from T1, R9-33, and LowBinder (Supplemental Table S2) was PCR-amplified (10 mM TRIS pH 8.3, 50 mM KCl, 1.5 mM $MgCl_2$, 0.1% gelatin, 200 μM each dNTP, 2.5 units *Taq* per 100 μL reaction, 0.5 μM primers) with primers 85.4 and 91.1 (Supplemental Table S2) using an annealing temperature of 50°C for 1.5 min. The primers added ClaI and SgrAI restriction sites, a T7 RNA polymerase promoter, a *lac* operator upstream of the mutant 6S RNA sequence, and an intrinsic terminator sequence immediately downstream from it. The three different DNA products were cloned into the pEcoli-Cterm 6xHN (Clontech) vector as described below (Supplemental Fig. S9). The DNA products for T1, R9-33, and LowBinder along with pEcoli-Cterm 6xHN vector were double-digested with ClaI and SgrAI (NEB). The vector was treated with CIAP (Roche), and ligation was carried out withT4 DNA ligase (Invitrogen) following the supplier's recommendations. Double-digested vector was ligated in the absence of insert, and the product (pEcoli-Empty) was used as an additional control during the in vivo analysis. Plasmids were transformed into *E. coli* BL21 (DE3) (Novagen) chemically competent cells containing a chromosomal copy of T7 RNA polymerase. Isolated colonies picked from LB+ Amp (100 μg/mL) plates were grown up overnight at 37°C in LB+ Amp broth with constant aeration (250 rpm). The next day, cells were diluted 1/100 into fresh LB+Amp with 5 mM IPTG, and the OD_{600} was measured every 60 min until all cultures entered stationary phase.

Cell culture

Single colonies of *E. coli* BL21 DE3 cells transformed with the different mutant constructs were picked from LB agar plates and grown ON in 1 mL LB or LB-Amp (100 μg/mL) at 37°C with constant aeration. The next morning cells were diluted 1/200, inoculated into fresh LB-Amp (100 μg/mL) in presence and absence of IPTG (5 mM) and incubated at 37°C with constant aeration. OD_{600} was measured every 60 min until all cultures entered stationary phase.

Colony survival assay

Single colonies of BL21 DE3 cells transformed with one of the following—pEcoli T1, pEcoli R9-33, pEcoli LowBinder or pEcoli-

Empty—were grown in LB+Amp (100 µg/mL) O/N at 37°C with constant aeration. The next day, cells were diluted 1/5 in fresh LB+Amp and incubated for another 2 h. Serial dilutions were prepared, and 50 µL of each dilution were spread on LB+Amp and LB+Amp +IPTG agar plates (done in triplicate). Plates were incubated O/N at 37°C. Colony-forming units (CFU/mL) were determined for each plasmid in the presence and absence of IPTG.

Northern blots

Aliquots of RNA (20 µg total RNA per lane for 8% denaturing gels) or cell extract (0.5 OD units per lane for 5% native gels) were blotted onto Hybond N+ nylon membrane (GE). Membranes were UV cross-linked using a Stratalinker (1200 µJ for 30 sec), and blocked, probed, and washed according to Krieg (Krieg 1996). For all Northern blots shown, in vitro-transcribed RNAs were used to confirm the absence of cross reactivity. Plasmids that were used as template for in vitro transcription were digested with ClaI and showed two RNA bands, with the larger corresponding to the runoff product of transcription.

SUPPLEMENTAL MATERIAL

Supplemental material is available for this article.

ACKNOWLEDGMENTS

P.J.U. acknowledges funding from NSERC, MSFHR, and the SFU Community Trust Endowment Fund.

Received January 13, 2014; accepted February 6, 2014.

REFERENCES

Borukhov S, Sagitov V, Josaitis CA, Gourse RL, Goldfarb A. 1993. Two modes of transcription initiation *in vitro* at the *rrnB* P1 promoter of *Escherichia coli*. *J Biol Chem* **268:** 23477–23482.

Cabrera-Ostertag IJ, Cavanagh AT, Wassarman KM. 2013. Initiating nucleotide identity determines efficiency of RNA synthesis from 6S RNA templates in *Bacillus subtilis* but not *Escherichia coli*. *Nucleic Acids Res* **41:** 7501–7511.

Cavanagh AT, Klocko AD, Liu X, Wassarman KM. 2008. Promoter specificity for 6S RNA regulation of transcription is determined by core promoter sequences and competition for region 4.2 of σ^{70}. *Mol Microbiol* **67:** 1242–1256.

Cavanagh AT, Sperger JM, Wassarman KM. 2012. Regulation of 6S RNA by pRNA synthesis is required for efficient recovery from stationary phase in *E. coli* and *B. subtilis*. *Nucleic Acids Res* **40:** 2234–2246.

Cheetham GM, Steitz TA. 1999. Structure of a transcribing T7 RNA polymerase initiation complex. *Science* **286:** 2305–2309.

Ederth J, Artsimovitch I, Isaksson LA, Landick R. 2002. The downstream DNA jaw of bacterial RNA polymerase facilitates both transcriptional initiation and pausing. *J Biol Chem* **277:** 37456–37463.

Hsu LM, Zagorski J, Wang Z, Fournier MJ. 1985. *Escherichia coli* 6S RNA gene is part of a dual-function transcription unit. *J Bacteriol* **161:** 1162–1170.

Jin DJ, Cagliero C, Zhou YN. 2012. Growth rate regulation in *Escherichia coli*. *FEMS Microbiol Rev* **36:** 269–287.

Kim KS, Lee Y. 2004. Regulation of 6S RNA biogenesis by switching utilization of both σ factors and endoribonucleases. *Nucleic Acids Res* **32:** 6057–6068.

Krieg PA. 1996. *A laboratory guide to RNA: isolation, analysis, and synthesis*. Wiley-Liss, New York.

Liu X, Martin CT. 2009. Transcription elongation complex stability: the topological lock. *J Biol Chem* **284:** 36262–36270.

Murakami KS, Darst SA. 2003. Bacterial RNA polymerases: the wholo story. *Curr Opin Struct Biol* **13:** 31–39.

Panchapakesan SS, Unrau PJ. 2012. *E. coli* 6S RNA release from RNA polymerase requires σ^{70} ejection by scrunching and is orchestrated by a conserved RNA hairpin. *RNA* **18:** 2251–2259.

Revyakin A, Liu C, Ebright RH, Strick TR. 2006. Abortive initiation and productive initiation by RNA polymerase involve DNA scrunching. *Science* **314:** 1139–1143.

Shephard L, Dobson N, Unrau PJ. 2010. Binding and release of the 6S transcriptional control RNA. *RNA* **16:** 885–892.

Steuten B, Wagner R. 2012. A conformational switch is responsible for the reversal of the 6S RNA-dependent RNA polymerase inhibition in *Escherichia coli*. *Biol Chem* **393:** 1513–1522.

Steuten B, Setny P, Zacharias M, Wagner R. 2013. Mapping the spatial neighborhood of the regulatory 6S RNA bound to *Escherichia coli* RNA polymerase holoenzyme. *J Mol Biol* **425:** 3649–3661.

Wassarman KM. 2007. 6S RNA: a small RNA regulator of transcription. *Curr Opin Microbiol* **10:** 164–168.

Wassarman KM, Saecker RM. 2006. Synthesis-mediated release of a small RNA inhibitor of RNA polymerase. *Science* **314:** 1601–1603.

Wassarman KM, Storz G. 2000. 6S RNA regulates *E. coli* RNA polymerase activity. *Cell* **101:** 613–623.